Journal of Fluorescence, Vol. 12, No. 2, June 2002 (© 2002)

Introduction of Fluorometry to the Screening of Protein Crystallization Buffers

Takamitsu Ikkai[1,3] and Katsuhiko Shimada[2]

Received February 26, 2002

A system to use fluorometry for the search of protein crystallization buffers was developed. The screening of candidates was done with a use of short gel-filtration column (Sephacryl S-100 HR) linked to the fluorometer. Protein elution was monitored by intrinsic fluorescence or emission from its labels. This method was applied to actin and actin complexes. When nuclei were formed in actin solution, preceding the peak of actin, a new peak appeared on the elution curve. It was found that the fluorescence allows detection of even small amount of nuclei formed in the buffer. Using the screened buffers, crystal growths were attempted. The images of crystals were captured by fluorescence microscope. The monitoring of nuclei with this method will accelerate the screening of crystallization buffers. This system is applicable to the crystallization of other proteins and their complexes.

KEY WORDS: Crystallization; short column; actin; DNase 1; rhodopsin.

INTRODUCTION

Crystal is indispensable for the understanding of protein structure and function. Its growth proceeds when nuclei are formed in the protein solution as a result of phase transition induced by precipitants. Dynamic light scattering (DLS) is often employed for the search of useful buffers in the initial stage of crystallization [1]. In this method the dispersity of aggregations is estimated with a decay analysis of autocorrelation function of the light scattered by a macromolecule undergoing Brownian motion. The globular proteins having comparatively low molecular weights are applied to this system [2], because the system works in the condition that the intensity of scattered light from an aggregate is small compared to the wavelength of light [1]. Crystals are grown from the buffers that induce monodisperse aggregation [3]. However, the applicability of crystals to the elongated molecules such as filaments formed by polymerization is as yet unclear. Usually in such a solution, the intrinsic scattering is high and the signal-to-noise ratio is low. Consequently, the unequivocal deconvolution of the diffusion coefficients for the different-size particles become difficult [4]. Another point is the fact that the sizes of aggregates and mobility are not determined uniquely from the diffusion coefficients. Sometimes the estimated distributions do not reflect the real sample distribution [5]. Here, an alternative method was developed for the filamentous molecules. It consists of the fluorometrical system based on the short column method. Previously concerning the use of gel-filtration column, the overestimate of monodispersity was implied, suggesting the sieving effect of the column as a cause [3]. The use of a short column seems to reduce this effect. In this system the dispersity is obtained as a profile of elution monitored by fluorescence. Fluorescence is effective to get signals selectively from the background noise. Provided appro-

[1] Aichi Prefectural University of Fine Arts Nagakute, Aichi 480-1194, Japan.
[2] School of Design and Architecture, Nagoya-City University Chikusaku, Nagoya 464-0083 Japan.
[3] To whom correspondence should be addressed. Tel: 81-593-31-5581. Fax; 81-593-31-3406. E-mail: ikkai@mail.aichi-fam-u.ac.jp

1053-0509/02/0600-0167/0 © 2002 Plenum Publishing Corporation

priate probes with high quantum yield are chosen, even small amounts of nuclei are monitored. This system was applied to actin. Actin is ubiquitous in almost all eukaryotic cells, and a large number of different proteins bind to actin. Actin forms filaments by polymerization and its scattering increases with polymerization [6]. We have shown previously the excess of ATP over actin caused polymerization [7]. This experience led us to try ATP as actin precipitant. This system worked well, and the nuclei formation was induced by ATP.

EXPERIMENTAL

Materials

Actin was extracted from rabbit skeletal muscle, and on a 2.5 × 80 cm column of Sephacryl S-100 HR, Pharmacia (Amersham Biosciences Co., Tokyo) was purified as described previously [8] in a low-salt A-buffer (0.1 m*M* ATP; 0.1 m*M* $CaCl_2$; 2 m*M* Tris-HCl, pH 8.0; and 1 m*M* NaN_3). The stock actin kept in A-buffer was filtered through 0.45-μ*M* pore filters, (MILLEX-HV; Millipore, Shinagawa, Tokyo) just before use. Polyethylene glycol 6000 (PEG) was obtained from Nacalai Tesque, Kyoto, Japan. DNase 1 was purchased from Worthington Biochemical Co. (Lakewood, NJ. USA). Rhodopsin was prepared from the eyes of squid (*Watasenia scintillans*), as described previously [9], in the presence of sucrose monolaurate (SM-1200) (DOJINDO Laboratory, Kumamoto, Japan). Labeling of actin in A-buffer with fluorescent probes *N*-(1-pyrene)iodoacetamide (PIA) (Molecular Probes, Eugene, OR, USA) or tetramethylrhodamine isothiocyanate (TMRITC) (Sigma-Aldrich, Tokyo) was done as described previously [10] in the presence of 10 times molar excess of probes over actin at 4°C in the dark for 30 min. The reaction was terminated with 20 m*M* 2-mercaptoethanol. The unreacted probes were removed using HiTrap Desalting column (Pharmacia) or dialysis. Images of crystals were recorded by CCD camera (Hamamatsu Photonics, Hamamatsu, Japan) mounted on the fluorescence microscope (Olympus BHA-RFL-LB, Tokyo) using 10× objective (NA:0.25). The fluorescence from 2′-(or-3′)-O-(*N*-methylanthraniloyl)-adenosine-5′-triphosphate (MANT-ATP) (Molecular Probes) bound to crystals was observed using a dichroic mirror DM400 and cutoff filters (UG-1 for excitation and L-435 for emission). The fluorescence from TMRITC-actin crystals was observed using a dichroic mirror DM580 and cutoff filters (BG-36 for excitation and O-570 for emission).

Fluorometry Using Short Column

The short column of 9 × 26 mm having a 20-μm pore filter at the one end was packed with Sephacryl S-100-HR (Pharmacia). Samples of 200 μL were eluted immediately with buffers at a rate of 0.5 ml/min. The eluate from the short column was fed through a polyethylene tube (2 mm in diameter) into a Hitachi F-2000 fluorometer equipped with a flow cell (90 μL). Throughout the experiments, the same short column was used.

Crystallizations of Actin

Using the buffer searched by the short column system, crystals were grown in capillaries of 2 × 100 mm. The end of the capillary was sealed with dialysis membrane with a cut-off of 8000 Da. About 20 μL of sample solution in the capillary was dipped in the test tube filled with 1.0 ml of buffer. Crystallizations of TMRITC-actin (4.3-mg/ml) were performed in buffer A. As a precipitant, 2m*M* ATP or MANT-ATP (final concentration) was added to buffer A.

RESULTS AND DISCUSSION

Fluorometric Detection of Nuclei in Actin Solution

Fig. 1A shows the effect of salts on actin observed by elution profiles. The elution of actin was monitored by intrinsic fluorescence at the emission of 333 nm. The intrinsic fluorescence of tryptophan on actin was used previously in monitoring the polymerization of actin [11]. Actin polymerizes in the presence of salts, e.g., 0.1 M NaCl. As shown in Fig. 1A, both types of actin, one in the monomeric state (curve a) and the other in the polymeric state (curve b) eluted from the short column almost in the same manner and the peaks had the same retention time. As shown here, the fluorescence intensity of the peak of actin in the presence of salts (curve b) was 25% lower compared to the peak of actin in the low-salt A-buffer (curve a). Because tryptophan fluorescence on actin is reduced 25% in the polymerized state compared to the monomeric actin in A-buffer [11], the actin in the short column was in the state of polymerized form.

Next, the ATP effect on actin as a precipitant was examined. ATP induces polymerization of actin in a low-salt buffer [7,12], thus, it may also cause the phase transition of actin resulting in nuclei formation. Here, instead of ATP, MANT-ATP was used to monitor the binding of ATP to actin. Curve c in Fig. 1A shows the elution profile of MANT-ATP observed at the emission of 447 nm. Actin

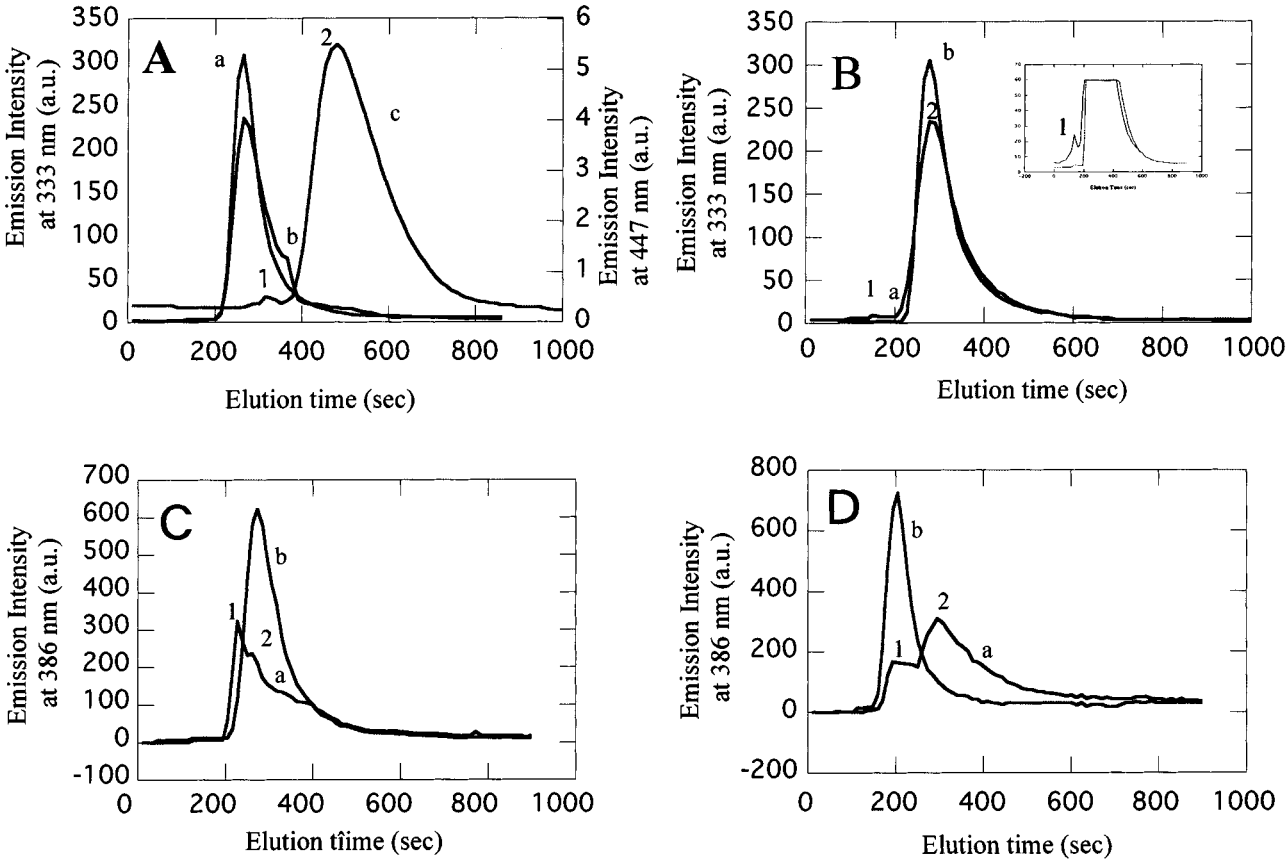

Fig. 1. (A) Comparisons of the elution profiles of actin monitored by fluorescence of MANT-ATP to those monitored with intrinsic fluorescence of actin. Actin concentrations were 5 μ*M*. Samples were eluted with Ca-buffer (0.1 m*M* $CaCl_2$; 1 m*M* NaN_3; 2 m*M* Tris-HCl, pH 8.0). Intrinsic fluorescence of tryptophan; excitation at 281 nm and emission at 333 nm (curves a and b). MANT-ATP fluorescence; excitation at 356 nm and emission at 447 nm (curve c). **a:** actin in low-salt A-buffer (see Material Section). **b:** actin in A-buffer was polymerized with additions of salts to 0.1 *M* NaCl and 2 m*M* $MgCl_2$ 30 min before application to the column. **c:** Immediately after addition of 1 μ*M* of MANT-ATP (final concentration), actin in A-buffer was applied to the short column and run. (B) Elution patterns of actin (5 μ*M*) from the short column observed by intrinsic fluorescence. Excitation at 281 nm and emission at 333 nm. Immediately after addition of 25 μ*M* MANT-ATP, actin in A buffer was applied to the column and run. **a:** in the presence of MANT-ATP. **b:** in the absence of MANT-ATP. Inset: the lower parts of the curves were enlarged to show clearly the nuclei formation. (C) Elution profiles of PIA-actin*DNase 1 complexes eluted with I-buffer (50 m*M* imidazol pH 6.6, 0.1 m*M* $CaCl_2$, 1 m*M* NaN_3). **a:** Just before elution, 10% PEG 6000 (final concentration) was added to the sample. **b:** No addition. Excitation is 344 nm and emission is 386 nm. (D) Elution patterns of PIA-actin*rhodopsin mixtures eluted with I-buffer in the presence of 0.1% sucrose monolaurate (SM-1200). **a:** Just before the elution, 10% PEG 6000 (final concentration) was added to the sample. **b:** no addition. Excitation is 344 nm and emission is 386 nm.

in the presence of 1 μ*M* of MANT-ATP showed a small peak (peak-1), which came out in advance of the main peak of MANT-ATP (peak-2). The position of peak-1 is included in the time range of actin elution observed on the curve a. From this result it is seen that a part of MANT-ATP was bound on actin. Because no actin elution was observed in the time range between 400 and 700 on the curve a, the large peak-2 on curve c will correspond to the elution of free MANT-ATP (or its product). Here, the peak corresponding to nuclei was not observed on curve c, i.e., any leading peak to peak-1 was not present. It is possible that the hydrolysis of MANT-ATP by actin might have released MANT-ATP from nuclei [12]. Then further a search to find nuclei induced by MANT-ATP was performed using intrinsic fluorescence of actin at the emission of 333 nm. Here, the concentration of MANT-ATP was increased to 25 μ*M*, resulting in 5-fold molar excess of MANT-ATP over actin. As shown in Fig. 1B the peak of curve a was 24% lower compared to that of curve b. This showed the polymerization of actin. Further, preceding to the main peak-2, the small peak-1 was observed on the curve a. This peak-1 is shown with enlargement on the inset. Comparing this peak-1 to the peak of curve b in Fig. 1A, it is seen that peak-1 eluted

in advance of the polymerized actin. This result shows that peak-1 was composed of aggregates having larger molecular sizes than those of the polymerized actin. Consequently, peak-1 represented the nuclei induced by MANT-ATP. As shown here, even the small amount of nuclei could be detected by this fluorometric system. Next, using ATP as a precipitant, crystals were grown. Crystals were observed with fluorescence microscope. As shown in Fig. 2, the fluorescence from actin crystals was monitored using the emissions from MANT-ATP (Fig. 2A) and TMRITC (Fig. 2B). The images by both emissions overlapped. This result confirmed the binding of MANT-ATP to actin. Consequently, the buffer A containing excess ATP over actin worked as precipitant. This result is new. So far it on the role of ATP in crystallization of actin has not been reported.

Searches of Nuclei in the Solution of Actin Complexes

Fig. 1C shows the elution profiles of actin*DNase 1. Using the buffer published for crystallization of actin*-DNase 1 [13], searches of aggregates were carried out. In the presence of precipitants (PEG 6000), a new peak appeared on the curve a, although it was not observed in the absence of precipitant (curve b). The leading peak-1 was higher compared to peak-2. This suggests that a large amount of nuclei was formed. Fig. 1D shows the elution profiles of actin*rhodopsin solution. Because rhodopsin is insoluble in water, sucrose monolaurate (SM-1200) was added to I-buffer. The rise of peak-1 corresponding to the nuclei on curve a suggests the usefulness of this buffer for crystallization of actin*rhodopsin. In this case, the peak-1 on curve a was not so high as that on curve a in Fig. 1C. So, the amount of nuclei seems to be lower compared to that in actin*DNase 1 solution. As shown here, short column worked for the search of nuclei without sieving, desalting and dilution to excess. Compared to the long column, the time of loading and elution of samples were spared. Even viscous samples such as long actin filaments [6] could be applied to it (Fig. 1A). Unlike DLS, molecular sizes of aggregates to be applied to it are not restricted by the wavelength of light. The fraction of monodisperse aggregates obtained from the short col-

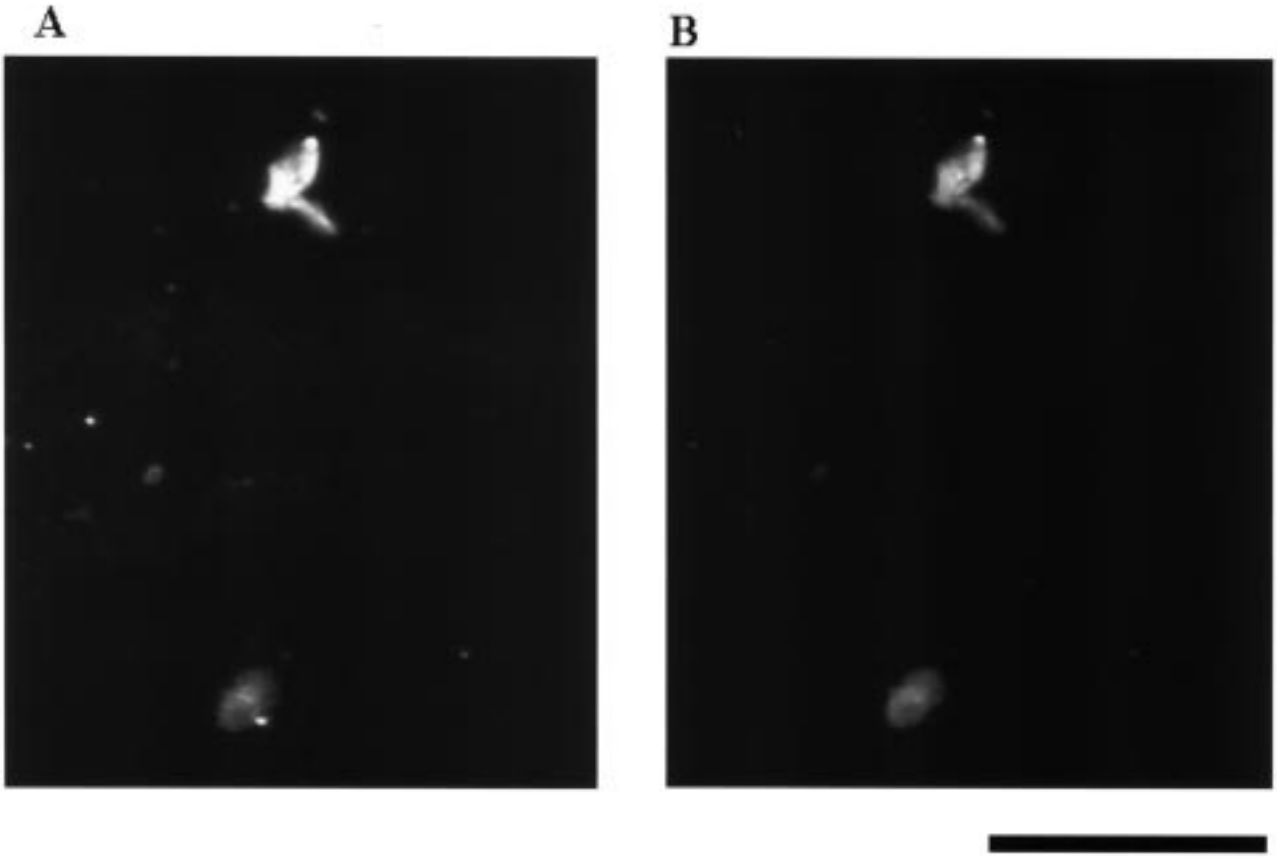

Fig. 2. Actin crystals observed by fluorescence microscope. Images were recorded by CCD camera. (a) Monitored by fluorescence of MANT-ATP. (b) Monitored by fluorescence of TMRITC. Bar shows 0.1 mm. Crystals were grown in the capillaries.

umn will be used for crystallization as a seed. Finally, for the search of buffers using samples from other sources, according to their molecular sizes, the length of column can be adjusted.

CONCLUSION

The search of crystallization buffers using a fluorometric system based on the gel-filtration through the short column was effective. With this system, ATP was found to be the precipitant of actin. In the fluorescence the monitoring of aggregates is possible with either a sample or precipitant. The selectiveness in this system accelerates the search of buffers for crystallization. The formation of nuclei was observed from the profile of gel-filtration. The molecular sizes of aggregates to be applied to this system can exceed the limitation to DLS.

ACKNOWLEDGMENTS

We are grateful to Dr. Koichi H. Kato (The Center of Natural Science, Nagoya-City University) for his favor to us concerning the access to CCD camera.

REFERENCES

1. Z. Kam, H. B. Shore, and G. Feher (1978). *J. Mol. Biol.* **123**, 539–555.
2. M. Skouri *et al.* (1991) *FEBS Lett.* **295**, 84–88.
3. A. R. Ferre-D'Amare and S. K. Burley (1997) *Meth. Enzymolo.* **276**, 157–166.
4. J. D. Donovan, G. B. Benedek, and M. C. Carey (1987) *Biochemistry* **26**, 8116–8125.
5. W. Kadima *et al.* (1990) *Biophys. J.* **57**, 125–132.
6. J. A. Cooper and T. D. Pollard *Methods Enzymol.* **85** 182–233.
7. T. Ikkai and K. Kondo (2000) *IUBMB Life* **49**, 77–79.
8. T. Ikkai and H. Kondo (1995) *Biochem. Mol. Biol. Int.* **37**, 1153–1161.
9. K. Kashima, M. Seidou, and Y. Kito (1978) *Biochim. Biophys. Acta* **536**, 78–87.
10. T. Ikkai and H. Kondo (1996) *J. Biochem. Biophys. Meth.* **33**, 55–58.
11. L. D. Selden, H. J. Kinosian, J. E. Estes and L. C. Gershman (1994) in J. E. Estes and P. J. Higgins (Eds.) *Advances in Experimental Medicine and Biology*, pp. 51–57 Plenum Press, New York.
12. T. Ikkai and K. Shimada (2000) *J. Fluoresc* **10**, 77–79.
13. W. Kabsch, H. G. Mannherz, D. Suck, E. F. Pai, and K. C. Holmes (1990) *Nature* **347**, 37–44.